IEEE Access
Multidisciplinary : Rapid Review : Open Access Journal

Received 13 October 2024, accepted 11 November 2024, date of publication 14 November 2024,
date of current version 25 November 2024.

Digital Object Identifier 10.1109/ACCESS.2024.3498437

RESEARCH ARTICLE

Artificial Neural Networks as a Natural Tool in Solution of Variational Problems in Hydrodynamics

IVAN STEBAKOV[1,2], ALEXEI KORNAEV[1,2], ELENA KORNAEVA[3], NIKITA LITVINENKO[1], YURI KAZAKOV[2], OLEG IVANOV[1,4], AND BULAT IBRAGIMOV[5]

[1]Research Center for Artificial Intelligence, Innopolis University, 420500 Innopolis, Russia
[2]Department of Mechatronics, Mechanics, and Robotics, Orel State University, 302026 Oryol, Russia
[3]Department of Information Systems and Digital Technologies, Orel State University, 302026 Oryol, Russia
[4]Higher School of Digital Culture, ITMO University, 197101 Saint Petersburg, Russia
[5]Department of Computer Science, University of Copenhagen, 1165 Copenhagen, Denmark

Corresponding author: Ivan Stebakov (i.stebakov@innopolis.ru)

The work of Ivan Stebakov, Alexei Kornaev, Nikita Litvinenko, and Oleg Ivanov were supported by the Analytical Center for the Government of Russian Federation under Agreement 70-2021-00143 01.11.2021 and Agreement IGK 000000D730324P540002.

ABSTRACT Artificial neural networks are a powerful tool for spatial and temporal functions approximation. This study introduces a novel approach for modeling non-Newtonian fluid flows by minimizing a proposed power loss metric, which aligns with the variational formulation of boundary value problems in hydrodynamics and extends the classical Lagrange variational principle. The method is distinguished by its data-free nature, enabling problem-solving through 2D or 3D images of the flow domain. Validation was performed using both multi-layer perceptrons and U-Net architectures, with results compared against analytical and numerical benchmarks. The method demonstrated good results with a relative error of 1.41% in comparison with the analytical solution for non-Newtonian fluids. The power loss formulation offers a clear advantage by simplifying the modeling process and enhancing interpretability. Notably, the proposed method demonstrates improvements over existing techniques by providing algorithmic simplicity and universality, with applications ranging from blood flow modeling in vessels and tissues to broader hydrodynamic scenarios.

INDEX TERMS Physics-based machine learning, calculus of variations, hydrodynamics, non-Newtonian fluids.

I. INTRODUCTION

The concept of minimizing effort has deep historical roots and finds resonance in both personal narratives and empirical observations [1]. Within the domain of continuum mechanics, fundamental principles are encapsulated by conservation laws, which manifest as variational principles. Notably, certain boundary value problems involving partial differential equations (PDEs) can be reformulated as variational problems [2], [3]. A significant challenge in employing direct methods from the calculus of variations lies in approximating unknown functions, particularly those involving multiple variables. The potential of artificial neural networks in addressing this challenge warrants detailed exploration [4], [5], [6]. This study leverages the generalized Lagrange variational principle to overcome the constraints imposed by non-Newtonian fluid properties and complex boundary conditions.

The associate editor coordinating the review of this manuscript and approving it for publication was Su Yan.

II. RELATED WORKS

The typical approaches to solving boundary value problems in hydrodynamics are based on various grid methods of computational fluid dynamics (CFD), including finite difference, control volume, and finite element methods [7], [8], [9], [10].

Another approach involves studying fluid flow characteristics as a fitting problem based on physical experiment data or CFD solution. This approach can be combined with a wide range of deep learning models, including long short-term memory (LSTM) networks, convolutional neural networks (CNN), and pre-trained generative transformers [11], [12]. However, due to the strong nonlinearity of the quantities under study, a large number of measurements are required, which is often challenging [13], [14], [15]. A relatively new approach involves the application of artificial neural networks to minimize residuals in differential equations. Kissas et al. [16] developed physics-informed neural networks (PINNs) to model blood flow in large and medium-sized vessels. Despite recent advances, this approach has low interpretability and generalizability [17]. Additionally, it requires a large number of calculated points for the dataset, as well as the previously mentioned problem with mesh generation for complex flow geometries [18]. Zhang et al. [19] applied convolutional neural networks to model homogeneous and heterogeneous Darcy flows, comparing the accuracy and efficiency of a PINN with the finite volume method (FVM). Ouyang et al. [20] used a chain-style physics-informed neural network (chain-style PINN) to model the cavitation effect. Aliakbari et al. [21] presented an approach to modeling hydrodynamic flows by calculating low-precision data using computational fluid dynamics (CFD) programs and then using PINN to obtain an accurate solution. Kumar et al. [22] presented an algorithm using a data-redundant deep neural network to simulate fully developed flows of non-Newtonian fluids, with complex rheological properties approximated using the Herschel-Bulkley model. The results demonstrated an average error of 11.5%. Sun et al. [18] presented a similar approach to modeling without using a training set, employing a multilayer perceptron (MLP) to approximate the pressure and velocity fields. The loss function, as in [21], was represented by the sum of the PDE residual of Eqs.(1, 2) with the addition of boundary and initial conditions. A similar work was presented by Li et al. [23], who solved the Reynolds equation in the region between two eccentric cylinders. PINN deals with the calculation of PDE components. Fully connected neural network (FCNN) based architectures allow the use of automatic differentiation for this purpose [24]. Also, for PINN, the following models are used: Fourier Feature Networks [25], Deep Galerkin Method (DGM) [26], deep operator networks (DeepONets) [27]. However, for deep learning methods based on LSTM, CNN, etc., the application of automatic differentiation is hindered by their structure and computational complexity. Automatic calculation of partial derivatives can be replaced by the use of finite difference schemes [28]. Most approaches based on PINN require retraining for each new case. However, some approaches allow obtaining a solution for a certain set of cases. Alexander Isaev et al. [29] consider modeling the flow in idealized four-vessel junctions, taking into account their geometry. For this purpose, parameters describing the geometry of the flow region are used as inputs to the FCNN. To solve non-stationary problems, the issue of time extrapolation can be considered. The original PINN does not cope well with this task. However, recent studies show the possibility of modifying PINN for extrapolation. Fesser et al. [30] noted the positive effect of transfer learning for extrapolation. Wang et al. [31] proposed Extrapolation-driven Deep Neural Networks (E-DNN), which significantly reduces the extrapolation error. Cuomo et al. [32] presented a solution to the Dirichlet problem for the Laplace equation, adding a constant heat flux as boundary conditions. The approach to minimizing the loss function, which has physical meaning, can be applied to the mechanics of solid [33] and deformable [3] bodies, as well as to fluid mechanics [34], [35]. The Lagrange variational principle [2] allows modeling fluid flows but has the following limitations: 1) the fluid is Newtonian; 2) the unknown functions and their first derivatives are fixed on the boundary; 3) both static and kinematic boundary conditions are required to find the value of the external power; 4) inertial and mass forces are negligible.

III. MATHEMATICAL MODELING

It is assumed that the fluid is incompressible and the flow is laminar and either stationary or quasi-stationary. Incompressibility is a natural property of fluids, while the assumptions of laminarity and stationarity are typical in hydrodynamics [36] and in the calculus of variations [1], respectively.

A. BOUNDARY VALUE PROBLEM FORMALIZATION

The Stokes equation and the incompressibility condition are under study [37], [38], respectively:

$$\nabla\cdot\mathbf{T}_\sigma = 0, \tag{1}$$
$$\nabla\cdot\mathbf{V} = 0, \tag{2}$$

where $\nabla\cdot\mathbf{T}_\sigma$ and $\nabla\cdot\mathbf{V}$ are the divergences of the stress tensor $\mathbf{T}_\sigma$ with the components σ_{ij}, $(i,j = 1\ldots3)$ and the velocity vector $\mathbf{V}$ with the components v_i, respectively.

The stress tensor components σ_{ij} can be expressed from the generalized Newtonian hypothesis [39], [40]:

$$\mathbf{D}_\sigma = 2\mu\mathbf{D}_\xi, \tag{3}$$

where $\mathbf{D}_\sigma = \mathbf{T}_\sigma - p\mathbf{T}_\delta$ is the deviator of the stress tensor with the components $[[s_{ij}]]$, p is the pressure, $\mathbf{T}_\delta$ is the unit tensor with the components $[[\delta_{ij}]]$, μ is the viscosity, $\mathbf{D}_\xi = [[\xi_{ij}]]$ is the strain rate tensor deviator part, the deviator is equal to the strain rate tensor $\mathbf{D}_\xi = \mathbf{T}_\xi$ for the incompressible fluids (Eq. 2).

Finally, the strain rate tensor can be calculated using Cauchy's formula [36], [38], [41]:

$$\mathbf{T}_\xi = (\nabla\otimes\mathbf{V} + \mathbf{V}\otimes\nabla)/2, \tag{4}$$

where $\nabla\otimes\mathbf{V}$ is the gradient of a vector function with components $\partial v_j/\partial x_i$.

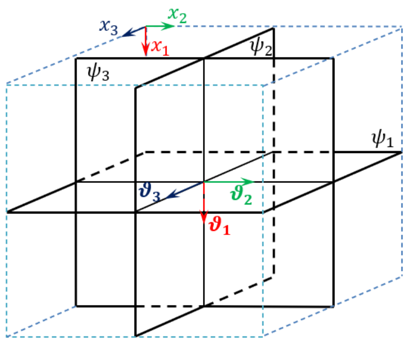

FIGURE 1. The unknown stream function with the components $[\psi_1(x_2, x_3), \psi_2(x_1, x_3), \psi_3(x_1, x_2)]$ and the velocity function **V** (Eq. 8) in the flow domain ($x_i^- \le x_i \le x_i^+$) of size [l_i].

So, the boundary value problem includes 4 scalar equations Eq. 1, 2 with 4 unknown functions: v_i, p. The boundary conditions (kinematic, static, mixed) are required to solve the problem.

B. VARIATIONAL PROBLEM AND THE LOSS FORMALIZATION

It is necessary to find a kinematic function that characterizes the velocity distribution within the flow domain (see Fig. 1) and minimizes a power functional. To extend the applicability of the Lagrange variational principle [2], [35], [42] and streamline the process of data labeling, the following variational principle is proposed:

$$J_L[\Psi] = \int_\Omega \Pi_v d\Omega + \lambda R \rightarrow min, R$$
$$= \int_{\Omega_w} (\nabla \times \Psi) \cdot (\nabla \times \Psi) d\Omega_w, \tag{5}$$

where where $\vartheta = [\psi_i(x_j)]$ is the unknown stream function ($i, j = 1, 2, 3$), Ω is the flow domain ($x_i^- \le x_i \le x_i^+$) with surface S that is characterized by a unit outer normal vector $\boldsymbol{n}$, $\Pi = \int T dH$ is the viscoelastic potential, $T = \sqrt{1/2 s_{ij} s_{ij}}$[1] is the shear stress intensity, $H = \sqrt{2\xi_{ij}\xi_{ij}}$ is the shear strain rate intensity, λ is a multiplier [1], $R = R(\psi_i(x_j))$ is the constrain that ensures the zero values for the velocity inside and on the surface of the solid region Ω_w of the flow domain Ω.

It can be shown using Euler equation [1] that the proposed principle Eq. 5 is true if the non-Newtonian properties of fluids are satisfied by the Herschel-Bulkley model [43], [44]:

$$\mu(H) = q_0 + q_1 H^{z-1}, \tag{6}$$

where q_0, q_1, z are the parameters obtained from rheological tests,

and the unknown Ψ function and its first partial derivatives are fixed on the surface S ($x_i = x_i^-, x_i = x_i^+$) of the flow domain Ω. The last point is equivalent to the boundary conditions [1].

Taking into account that the generalized Newtonian hypothesis can be converted into the following form: [40]:

$$T = \mu H, \tag{7}$$

and the velocity **V** is a vorticity of the unknown Ψ function:

$$\mathbf{V} = \nabla \times \Psi, \tag{8}$$

the functional 5 depends on one unknown function ϑ. In this work the 3D velocity distribution Eq. 8 depends on 3 2D scalar functions that are the components of the Ψ function. It should be noted, that the velocity distribution is solenoidal [42]. So, the incompressibility condition [38], [41] is true, that makes any Ψ function kinematically admissible in the flow domain. The Ψ function and its derivatives are fixed on the surface S of the flow domain Ω, and constrained in the solid regions of the flow domain Ω_w, if any. The unknown function Ψ can be represented in the discrete form and the proposed variational principle Eq. 5 can be minimized by means of artificial neural networks. This allows non-Newtonian fluid flows modeling.

C. NUMERICAL DIFFERENTIATION AND INTEGRATION

Both the 'autograd' built-in functions and finite differences are applied for the approximation of derivatives [42]. Templates of 5 or 3 points for polynomials of fourth or second degree, respectively, are used. The Simpson's rule is applied for numerical integration [42].

IV. DATA COLLECTION

The proposed method is data set free; instead, it utilizes a single image to inform the flow domain configuration and determine the boundary conditions of the problem. Both synthetic and medical images are employed in this study and are compiled into a toy data set [45]. Some images are sourced from the Vascular Model Repository (VMR) [46], which includes image data, pathlines, segmentations, models, inflow rates, and simulation results for various large blood vessels. All segmentations, models, and simulation results in VMR were generated using SimVascular [47] and have been clinically validated. Given that the image volumes in VMR exhibit anisotropic pixel spacing, we resampled certain volumes to ensure uniform spacing in all directions.

V. SIMULATION MODELING

Based on the mathematical models described above, a series of simulation models were conducted: models based on the boundary value problem analytical or numerical solution (models 0, M0); models based on the generalized Lagrange functional Eq. 5 minimization (models 1, M1). The code and the toy data set are available on the repository [45].

A. BOUNDARY VALUE PROBLEM SOLUTION (M0)

Obviously, analytical solutions can be found for the simplest or asymptotic cases. Particular case of a 2D flows of a non-Newtonian fluid Eq. 6 between two parallel plates has known analytical solutions [48] that were implemented for Newtonian, dilatant, pseudo plastic and Bingham fluids [45]. In this work we also designed a simulation model [45] for an MLP based PINN model that solves the boundary value problem presented in section III-A of

[1]The Einstein summation notation is used in this work.

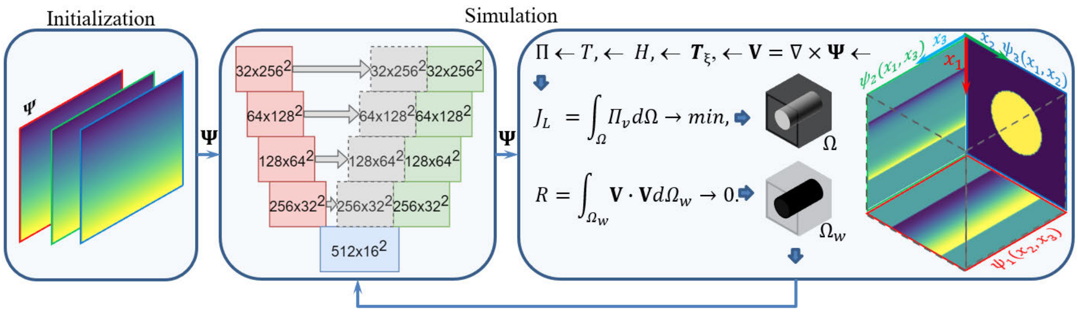

FIGURE 2. Visualization of the 3D fluid flow simulation model (M1) based on minimization of the generalized Lagrange functional (Eq. 5). Image-based approach is implemented with U-Net. The model receives three initial images (e.g. random noise) of the unknown functions $\psi_1(x_2, x_3)$, $\psi_2(x_1, x_3)$, $\psi_3(x_1, x_2)$, then generates the unknown functions and calculates loss (Eq. 5). 3D image of the flow domain is used as mask when calculating loss. During the training, the network approaches the unknown functions to the solution of the problem.

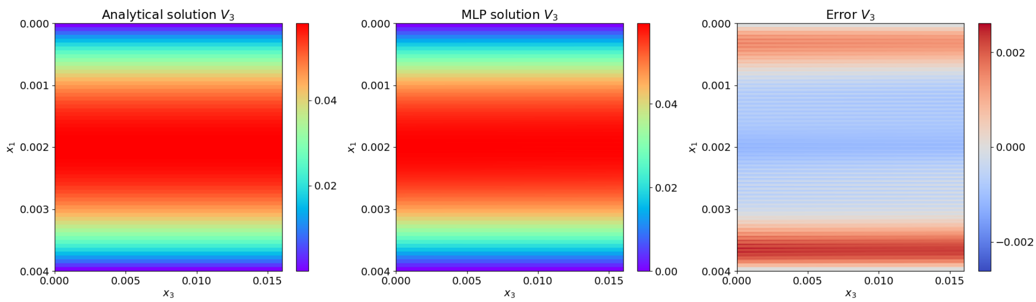

FIGURE 3. Comparison of the analytical and numerical solution using domain-based and MLP for the non-Newtonian fluid.

the paper. The model is based on known algorithms that minimize residual of the equations of the mathematical model (see section III-A) and take the boundary conditions into account [19], [20], [22], [49].

B. GENERALIZED LAGRANGE FUNCTIONAL MINIMIZATION (M1)

The proposed method of fluid flow modeling is based on a power loss minimization and it was implemented with image-based approach and domain-based approach for the cases of 2D and 3D flows of non-Newtonian fluids Eq. 6.

1) IMAGE-BASED APPROACH WITH U-NET

The model was implemented with U-Net [50], [51]. The model operates with the pixel values that correspond to the values of the unknown Ψ function. The U-Net receives 3 images of 3 components of the unknown function ϑ. Random noise can be applied or projections of the flow domain mask. To fulfill the boundary conditions of the ϑ function on the walls, the required values are written directly into the predicted tensor. To fulfill the boundary conditions of the velocity on the walls, an additional component is introduced into the loss function. The MSE loss function is used to calculate this component. Each component is multiplied by a weighting factor. These coefficients are the hyperparameters of the model. In hidden layers, the ReLU activation and batchnorm are used. The output uses the sigmoid activation function, which fixes the psi function in a given range. The Adam method is used for optimization.

Algorithm 1 Image-Based Approach to 2D Fluid Flow Modeling (M1)

Input: image of the flow domain, *img*, image size s [1,*s*,*s*]; number of epochs, E; hyperparameters, *hyps*; flow domain sizes along coordinates x_i ($i = 1 \ldots 3$), [l_i]; viscosity model parameters: q_0, q_1, z; flow rate, Q_3; number of boundary layers, NL.
Output: $\Psi = [0, \psi_2, 0]$ function in the form of image of ψ_2

Initialize Ψ function and parameters of the U-Net, Θ_0; binarize image of the flow domain, *img*.
$\mathbf{X} \leftarrow \psi_2$
for $e \leftarrow 1, E$ **do**
  $\psi_2 \leftarrow U - Net(\mathbf{X}, \Theta)$
  $\psi_2 \leftarrow$ *apply the boundary conditions*, ψ_2[:NL,:] = 0, ψ_2[-NL:,:] = Q_3/L_2
  $\mathbf{V}, \mathbf{T}_\xi$,H, $\Pi \leftarrow$ *applynumericaldifferentiationof* ψ_2
  $J \leftarrow$ *applynumericalintegrationof* Π, ψ_2
  $J_{V_0} \leftarrow$ *applyMSELosstoV on walls*
  $J_{overall} \leftarrow W_J \cdot J + W_{V_0} \cdot J_{V_0}$
  $\Theta, \lambda \leftarrow$ *update the parameters to minimize the loss*
end for

The algorithm 1 for the case of 2D flows is presented below. The algorithm can be relatively easy generalized for

Algorithm 2 Domain-Based Approach to 2D Fluid Flow Modeling (M1)

Input: image of the flow domain, *img*, image size s [1,s,s]; number of epochs, E; hyperparameters, *hyps*; flow domain sizes along coordinates x_i ($i = 1\ldots3$), [l_i]; viscosity model parameters: q_0, q_1, z; flow rate, Q_3.
Output: $\Psi = [0, \psi_2, 0]$ function in the form of image of ψ_2

```
Initialize parameters of the MLP, Θ0; binarize image of
        the flow domain, img.
Generate input X from domain sizes.
for e ← 1, E do
    ψ2 ← MLP(X, Θ)
    V, Tξ ,H, Π ← applyautomaticdifferentiationof ψ2
    J ← apply automatic integration of Π, ψ2
    J_V0 ← applyMSELosstoV  on walls
    J_ψ ← applyMSELosstoψ2 on walls
    J_overall ← W_J · J + W_V0 · J_V0 + J_ψ · W_ψ
    Θ, λ ← update the parameters to minimize the loss
end for
```

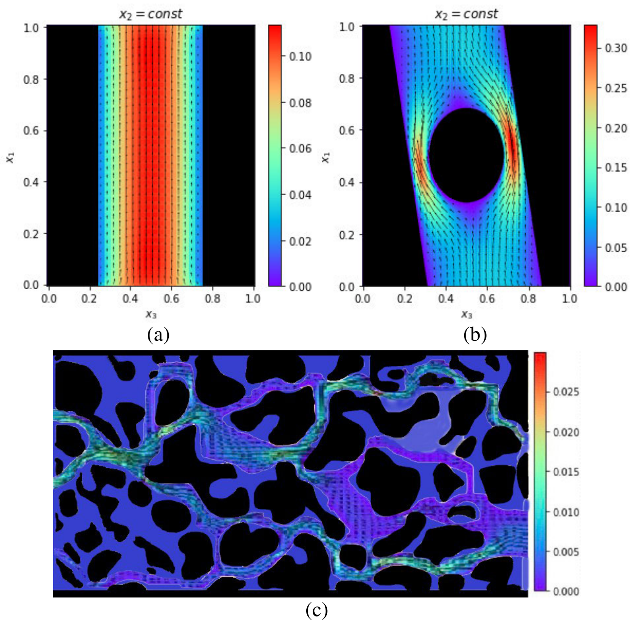

FIGURE 4. Visualization of the velocity distribution in flow domains between two parallel plates (a), parallel plates with cylinder (b), and inside the porous media.

the case of 3D flows since the mathematical model described in the previous section is general.

In case of 2D flows the unknown function has one non-zero component $\Psi = [0, \psi_2, 0]$. The scalar function $\psi_2 = \psi_2(x_1, x_3)$ that can be represented in the discrete form of an image or a matrix of size [s,s]. Then the velocity Eq. 8 has two non-zero components:

$$\mathbf{V} = \left[-\frac{\partial \psi_2}{\partial x_3},\ 0,\ \frac{\partial \psi_2}{\partial x_1}\right]. \tag{9}$$

It is supposed that the flow inlet and outlet are located on the surfaces S_3 ($x_3 = x_3^-$, $x_3 = x_3^+$) and the value of the flow rate Q_3 is known (see Fig. 1). Taking Eq. 9 into account the flow rate depends on boundary values of the unknown function:

$$Q_3 = \int\int_{S_3} v_3 \, dS_3 = (\psi_2^+ - \psi_2^-) l_2, \tag{10}$$

where ψ_2^-, ψ_2^+ are values of the unknown function on the boundaries $x_1 = x_1^-$ and $x_1 = x_1^+$, respectively, l_2 is the size of the flow domain along x_2 axis.

Since the ψ_2 function should have fixed values on the boundaries of the flow domain, the following boundary conditions should be met:

$$\psi_2(x_1 = x_1^-) = 0,\ \psi_2(x_1 = x_1^+) = Q_3. \tag{11}$$

The boundary conditions Eq. 11 make the flow rate fixed. It can be demonstrated that they are also equivalent to static boundary conditions on the surfaces S_3 since the flow rate is proportional to the pressure drop along x_3 axis.

The unknown ψ_2 function can be initialized in the form of linear distribution with fixed boundary values Eq. 11. Additionally, the function should have *NL* fixed boundary layers to satisfy requirement on zero derivatives of the unknown function on the boundaries.

The image of the flow domain can be both, gray scale or color, the only requirement is that the flow domain should be in white color. The image is binarized at the stage of preprocessing. The mask of the flow domain is necessary to calculate the constrain part of the loss Eq. 5. The flow domain size [l_i], the flow rate Q_3, the fluid properties Eq. 7 are also used as inputs of the model. The model has the following hyperparameters: image resolution s, number of epochs E, number of features of the network [51], learning rate and learning schedule, activation function of the output neurons (linear, sigmoid, hyperbolic tangent).

The basic U-Net architecture is known [51]. The output values of the network are normalized with ψ_2^+ value and the activation function is applied.

The network receives a mini-batch with initialized ψ_2 function in the form of tensor $[1, 1, s, s]$. The forward pass includes the following steps: the network outputs the corrected ψ_2 discrete distribution in the form of tensor $[1, 1, s, s]$.

Among all admissible Ψ functions, the true one or the nearest to the true one gives the loss Eq. 5 minimum value. The algorithm can be generalized for the case of 3D flows as it is shown in Fig. 2.

2) DOMAIN-BASED APPROACH WITH AN MLP

The model was also implemented with an MLP. The model operates with the coordinates of the flow domain and calculates the values of the unknown Ψ function in the nodes of the flow domain.

The algorithm 2 for the case of 2D flows is similar to the algorithm. The MLP receives the normalized values of the coordinates of each node. The loss can be calculated with automatic differentiation function. All the boundary conditions are implemented with the additional boundary

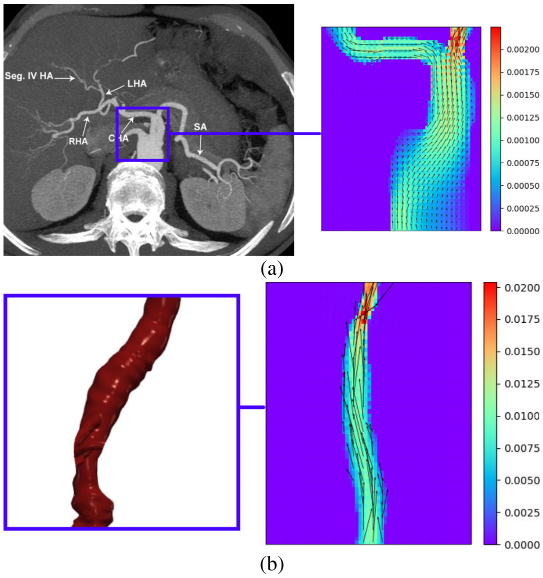

FIGURE 5. Visualization of the distribution of blood flow velocity in: common hepatic and splenic arteries on axial CT scan of the abdomen [52] (a), diagonal section of the abdominal aorta [46] (b).

conditions losses on the walls. The hidden layers have 'Tanh' activations. In cases of 3d flows each component of the unknown function has separate network.

VI. RESULTS AND DISCUSSION

The experiments were conducted on a personal computer equipped with an Intel Core i5-12400F CPU, an NVIDIA GeForce RTX 3060 GPU with 12GB of VRAM, 32GB of DDR5 RAM, and running Windows 11 operating system.

The main series of the simulation experiments deals with 2D flows of Newtonian and non-Newtonian fluids. Fluid flow between two parallel plates (see Fig. 4a) is a test task that allows to verify the accuracy of the proposed models. The other tasks demonstrate abilities of the models in processing of the synthetic and medical images. It is supposed that the fluid flows between two parallel plates. The flow domain size is [0.016, 0.016, 0.016] m and the gap is 0.004 m. Two types of fluids, Newtonian with the flow rate of $4e-6\ m^3/s$ and non-Newtonian with the flow rate of $2.57e-06\ m^3/s$, were under study. Both of the fluids are similar to blood. Whole blood is a two-phase liquid, composed of cellular elements suspended in plasma. Whole blood is a non-Newtonian fluid and characterized as shear-thinning, viscoelasticity, yield stress and thixotropy behavior [40], [53]. Many experimental studies have shown that blood is a predominantly shear thinning fluid [54], [55], [56], [57]. Taking the Herschel-Bulkley law Eq. 6 into account, the Newtonian and non-Newtonian fluids have the following rheological models, respectively: $\mu = 0.004\ Pa \cdot s$, $\mu = 0.132H^{0.801}\ Pa \cdot s$. The flow is laminar and steady, the Reynolds number is smaller than the critical one $Re < Re^*$.

Two models: MLP and U-Net were applied. MLP included 10 hidden layers with 20 neurons in the each layer. The input images resolutions were 128 and 256 pixels. Results were compared with analytical solutions 1.

TABLE 1. Results.

Model	SIZE	Fluid type	Simulation time, s	$max(v_3)$ error, %	$mean(v_3)$ error, %
MLP	128	Newtonian	150	4.57	4.37
MLP	128	Non-Newtonian	140	5.22	2.14
MLP	256	Newtonian	350	2.83	1.67
MLP	**256**	**Non-Newtonian**	**360**	**2.15**	**1.41**
U-Net	128	Newtonian	400	2.65	5.34
U-Net	128	Non-Newtonian	170	2.31	6.72
U-Net	256	Newtonian	600	0.76	4.8
U-Net	256	Non-Newtonian	700	1.31	4.89

In case of MLP model the type of fluid doesn't affect the accuracy of the model. The accuracy and the simulation time increase with increasing the resolution of the image. Fig. 3 demonstrates comparison of the simulation and analytical results.

In case of U-Net model the results are similar in general. The disadvantage of the U-Net model is simulation time. The mean error is relatively higher, but the maximum velocity values are calculated more accurate.

To demonstrate the goal of the proposed method, the series of additional tasks were performed: fluid flow between plates and cylinder and the flow through the porous media (see Fig. 4c). The flow domain of size [0.00032, 0.00032, 0.00064] m with the flow rate of $1e-9\ m^3/s$ was under study.

Despite the fact, that the blood flow in vessels correspond to the case of 3D flow, some of the CT image slices were used in simulation tests to demonstrate the ability of medical images processing. The flow domain of liver aorta of size [0.035, 0.02, 0.035] m and the abdominal aorta domain of size 0.15, 0.025, 0.15 with the flow rates of $2e-6\ m^3/s$ and $4e-5\ m^3/s$ were under study, respectively.

Fig. 6 demonstrates the simplest case of 3D fluid flow in a pipe. The results for the pipe has similar to the 2D tasks accuracy. But the accuracy decreases dramatically when the shape of the flow domain is complex. This is probably the result of the implementation of the unknown function components in the form of 2D functions.

Concluding the results it should be noted that the main hyperparameters of the proposed models are the multipliers of boundary conditions loss components. Their values can affect the convergence time and accuracy of the models. The difficulty lies in the manual selection of these multiplier. With the obtained values of the coefficients, it is possible to further change the type of fluid and the flow domain resolutions. However, the coefficients need to be adjusted if the flow rate or the flow domain geometry changes. Thus, methods of adaptive change of weight coefficients [58], [59] as well as methods of constrained optimization [60] may help to increase the efficiency and accuracy of the models. Further work is also associated with the development of a more flexible solution for 3D flow domains.

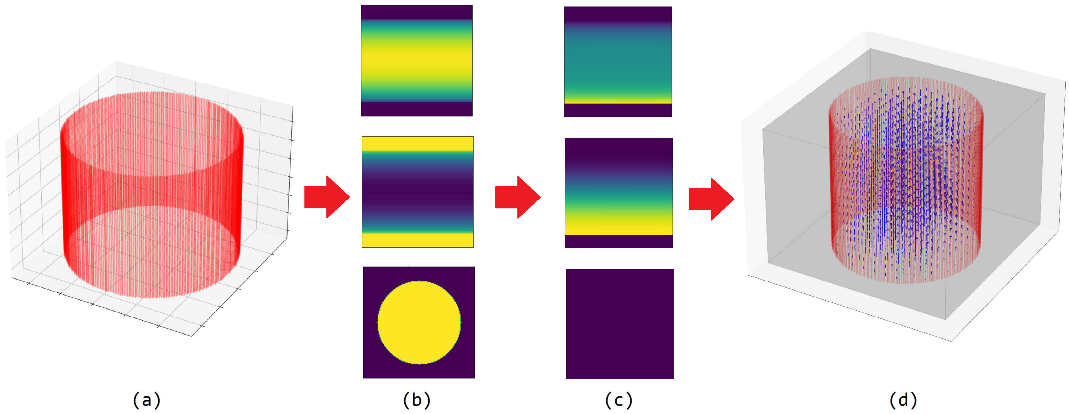

FIGURE 6. 3D flow in a pipe: domain mask (a), the unknown functions ψ_i initialization (b), and the simulation results for the unknown functions (c) and the velocity distribution V (d).

VII. LIMITATIONS

The variational approach faces general limitations in modeling stationary or quasi-stationary flows. While these limitations can be partially addressed by employing inequalities to obtain upper and lower bounds of variational solutions, such inequalities are beyond the scope of this study. The effects of turbulence or cavitation, which possess complex and stochastic natures, also fall outside the purview of this research. Implementing a variational approach for multiphysics tasks, such as flows with thermal effects or boundary deformations, can be challenging. However, hydrodynamics offers a set of criteria, including the Reynolds and Strouhal numbers, which help assess the significance of these effects during the conceptual formulation of problems.

VIII. CONCLUSION

The proposed method allows solution of the complex problems in hydrodynamics of non-Newtonian fluids with a simple tool based on machine learning and image processing. The method is data set free and the only image with the labeled flow domain is applied to determine the flow domain configuration and to satisfy the boundary conditions during the training.

The principal advantages of this method include its algorithmic simplicity, interpretability, and universality, enabling a broad spectrum of applications, such as the modeling of blood flow within vessels and tissues.

Conversely, the method exhibits several drawbacks: it is currently limited to stationary or quasi-stationary flows; it demands significant computational time and is highly sensitive to image resolution, owing to the reliance on differential methods.

APPENDIX

SUPPLEMENTARY MATERIAL

The proposed variational principle Eq. 5 includes the main part that is generalized Lagrange functional and the residual part that helps to satisfy the kinematic boundary conditions.

Original Lagrange variational principle depends on velocities v_i and pressure p function, has an additional term equal to the power of external forces in the form of the surface integral, and deals with Newtonian fluids. In this work we proposed the generalized Lagrange variational principle that depends on stream functions ψ_i and can be applied both to Newtonian and non-Newtonian fluids.

Fluid flow in the flow domain Ω with surface S characterized with unit outer normal vector $\mathbf{n}$ is under study. It is supposed, that the velocity distribution $\mathbf{V}$ is a vortex of an Ψ distribution: $\mathbf{V} = \nabla \times \Psi$. This distribution $\Psi = [\psi_i]$ is the unknown function.

A. LAGRANGE VARIATIONAL PRINCIPLE GENERALIZATION FOR THE 3D FLOWS OF NEWTONIAN FLUIDS

It is supposed, that the unknown functions ψ_i and the velocity components v_i are fixed on the boundary S. This is equivalent to the kinematic boundary conditions. It is also supposed that the viscosity has constant value $\mu = const$.

a: THEOREM:

the functional $J_L[\Psi] = \int_\Omega \Pi_v d\Omega$ has minimal value at the real Ψ distribution in comparison with any other Ψ' distribution that have fixed values and their first derivatives fixed values on the surface S of the flow domain Ω.

b: PROOF.

The functional has the following form for Newtonian fluids:

$$J_L[\Psi] = \frac{\mu}{2} \int_\Omega H^2 d\Omega = \frac{\mu}{2} \int_\Omega \mathbf{D}_\xi \cdot \mathbf{D}_\xi d\Omega. \tag{12}$$

The residual has the following form:

$$\mathbf{D}'_\xi \cdot \mathbf{D}'_\xi - \mathbf{D}_\xi \cdot \mathbf{D}_\xi = (\mathbf{D}'_\xi - \mathbf{D}_\xi) \cdot (\mathbf{D}'_\xi - \mathbf{D}_\xi) + 2(\mathbf{D}'_\xi - \mathbf{D}_\xi) \cdot \mathbf{D}_\xi. \tag{13}$$

The following equalities are known in the tensor calculus [42]:

$$\mathbf{D}_\xi \cdot \mathbf{D}_\xi = \mathbf{D}_\xi \cdot (\nabla \otimes \mathbf{V}),$$
$$\nabla \cdot (\mathbf{D}_\xi \cdot \mathbf{V}) = (\nabla \cdot \mathbf{D}_\xi) \cdot \mathbf{V} + \mathbf{D}_\xi \cdot (\nabla \otimes \mathbf{V})$$

$$\nabla \cdot [(\nabla \cdot \mathbf{D}_\xi) \times \Psi] = \Psi \cdot [\nabla \times (\nabla \cdot \mathbf{D}_\xi)] - (\nabla \cdot \mathbf{D}_\xi) \cdot (\nabla \times \Psi). \tag{14}$$

Taking the velocity distribution $\mathbf{V} = \nabla \times \Psi$ into account, the following equations are true:

$$\mathbf{D}_\xi \cdot \mathbf{D}_\xi = \nabla \cdot (\mathbf{D}_\xi \cdot \mathbf{V}) + \nabla \cdot [(\nabla \cdot \mathbf{D}_\xi) \times \Psi] - \Psi \cdot [\nabla \times (\nabla \cdot \mathbf{D}_\xi)], \tag{15}$$

$$2\mathbf{D}_\xi \cdot (\mathbf{D}'_\xi - \mathbf{D}_\xi) = 2\nabla \cdot (\mathbf{D}_\xi \cdot (\mathbf{V}' - \mathbf{V})) + 2\nabla \cdot [(\nabla \cdot \mathbf{D}_\xi) \times (\Psi' - \Psi)] - 2(\Psi' - \Psi) \cdot [\nabla \times (\nabla \cdot \mathbf{D}_\xi)]. \tag{16}$$

Taking the Newton law $\mathbf{D}_\sigma = 2\mu\mathbf{D}_\xi$ and Eq. 13, 14, 15, 16, residual of the functional 12 can be presented as follows:

$$J'_L - J_L = \mu \left(\int_\Omega (\mathbf{D}'_\xi - \mathbf{D}_\xi) d\Omega \right) + \int_S \mathbf{n} \cdot (\mathbf{D}_\xi \cdot (\mathbf{V}' - \mathbf{V})) dS + \int_S \mathbf{n} \cdot [(\nabla \cdot \mathbf{D}_\xi) \times (\Psi' - \Psi)] dS - \int_\Omega (\Psi' - \Psi) \cdot [\nabla \times (\nabla \cdot \mathbf{D}_\xi)] d\Omega. \tag{17}$$

The residual 17 has one non-zero positive value. So, residual is minimal for the true distribution Ψ.

B. KOROVCHINSKY VARIATIONAL PRINCIPLE GENERALIZATION FOR THE 3D FLOWS OF NEWTONIAN FLUIDS

1) FLOW BETWEEN TWO PARALLEL PLATES

It is supposed, that the Newtonian fluid flow is characterized with one-component velocity field:

$$\mathbf{V} = \left[0, \ 0, \ v_3(x_1, x_2)\right], \tag{18}$$

and the the unknown functions v_3, p depend on one parameter:

$$v_3 = v_3^* + \alpha(1 - x_1^2)(x_3 - x_3^3/3),$$
$$p = p^* + \beta(1 - x_1^2)(1 - x_3^2), \tag{19}$$

where $v_3^* = -\frac{1}{2\mu}\frac{\partial p^*}{\partial x_3}(1 - x_1^2)$ is the true velocity function (analytical solution of the task), $\frac{\partial p^*}{\partial x_3} = const$ is the true pressure drop along the flow direction x_3, $p^* = \frac{\partial p^*}{\partial x_3}(1 + x_3) + p_0$ is true pressure function, $p_0 = p^*(x_3 = -1)$ is given inlet pressure that is a static boundary condition, α, β are variable parameters of the model.

ACKNOWLEDGMENT

The authors want to acknowledge the assistance provided by AI-driven language processing tools, which have been instrumental in improving the grammatical accuracy and linguistic clarity of this work. The use of DeepSeek has refined the language in some sections, thereby enhancing the readability and overall quality of the article.

REFERENCES

[1] I. M. Gelfand and S. V. Fomin, *Calculus of Variations*. Little Falls, NJ, USA: Courier Corporation, 2000.
[2] R. S. Schechter and G. F. Newell, *The Variational Method in Engineering*, vol. 35. Little Falls, NJ, USA: American Society of Mechanical Engineers Digital Collection, Mar. 1968.
[3] E. Samaniego, C. Anitescu, S. Goswami, V. M. Nguyen-Thanh, H. Guo, K. Hamdia, X. Zhuang, and T. Rabczuk, "An energy approach to the solution of partial differential equations in computational mechanics via machine learning: Concepts, implementation and applications," *Comput. Methods Appl. Mech. Eng.*, vol. 362, Aug. 2019, Art. no. 112790.
[4] K. Hornik, M. Stinchcombe, and H. White, "Multilayer feedforward networks are universal approximators," *Neural Netw.*, vol. 2, no. 5, pp. 359–366, Jan. 1989.
[5] M. W. M. G. Dissanayake and N. Phan-Thien, "Neural-network-based approximations for solving partial differential equations," *Commun. Numer. Methods Eng.*, vol. 10, no. 3, pp. 195–201, Mar. 1994.
[6] N. Thuerey, P. Holl, M. Mueller, P. Schnell, F. Trost, and K. Um, "Physics-based deep learning," in *Proc. WWW*, 2021, pp. 233–236.
[7] J. Vimmr, A. Jonasova, and A. Jonásová, "On the modelling of steady generalized Newtonian flows in a 3D coronary bypass," *Eng. Mech.*, vol. 15, no. 3, pp. 193–203, 2008.
[8] T. Bodnár, A. Sequeira, and M. Prosi, "On the shear-thinning and viscoelastic effects of blood flow under various flow rates," *Appl. Math. Comput.*, vol. 217, no. 11, pp. 5055–5067, Feb. 2011.
[9] Y. H. Kim, P. J. Vandevord, and J. S. Lee, "Multiphase non-Newtonian effects on pulsatile hemodynamics in a coronary artery," *Int. J. Numer. Methods Fluids*, vol. 58, no. 7, pp. 803–825, Nov. 2008.
[10] C. Fisher and J. S. Rossmann, "Effect of non-Newtonian behavior on hemodynamics of cerebral aneurysms," *J. Biomechanical Eng.*, vol. 131, no. 9, Sep. 2009, Art. no. 091004.
[11] S. D. Yang, Z. A. Ali, H. Kwon, and B. M. Wong, "Predicting complex erosion profiles in steam distribution headers with convolutional and recurrent neural networks," *Ind. Eng. Chem. Res.*, vol. 61, no. 24, pp. 8520–8529, Jun. 2022.
[12] S. D. Yang, Z. A. Ali, and B. M. Wong, "FLUID-GPT (fast learning to understand and investigate dynamics with a generative pre-trained transformer): Efficient predictions of particle trajectories and erosion," *Ind. Eng. Chem. Res.*, vol. 62, no. 37, pp. 15278–15289, Sep. 2023.
[13] X. Jin, P. Cheng, W.-L. Chen, and H. Li, "Prediction model of velocity field around circular cylinder over various Reynolds numbers by fusion convolutional neural networks based on pressure on the cylinder," *Phys. Fluids*, vol. 30, no. 4, Apr. 2018, Art. no. 047105.
[14] R. Han, Y. Wang, Y. Zhang, and G. Chen, "A novel spatial–temporal prediction method for unsteady wake flows based on hybrid deep neural network," *Phys. Fluids*, vol. 31, no. 12, Dec. 2019, Art. no. 127101.
[15] P. A. Srinivasan, L. Guastoni, H. Azizpour, P. Schlatter, and R. Vinuesa, "Predictions of turbulent shear flows using deep neural networks," *Phys. Rev. Fluids*, vol. 4, no. 5, May 2019, Art. no. 054603.
[16] G. Kissas, Y. Yang, E. Hwuang, W. R. Witschey, J. A. Detre, and P. Perdikaris, "Machine learning in cardiovascular flows modeling: Predicting arterial blood pressure from non-invasive 4D flow MRI data using physics-informed neural networks," *Comput. Methods Appl. Mech. Eng.*, vol. 358, Jan. 2020, Art. no. 112623.
[17] Y. Li, J. Chang, C. Kong, and W. Bao, "Recent progress of machine learning in flow modeling and active flow control," *Chin. J. Aeronaut.*, vol. 35, no. 4, pp. 14–44, Apr. 2022.
[18] L. Sun, H. Gao, S. Pan, and J.-X. Wang, "Surrogate modeling for fluid flows based on physics-constrained deep learning without simulation data," *Comput. Methods Appl. Mech. Eng.*, vol. 361, Apr. 2020, Art. no. 112732.
[19] Z. Zhang, X. Yan, P. Liu, K. Zhang, R. Han, and S. Wang, "A physics-informed convolutional neural network for the simulation and prediction of two-phase Darcy flows in heterogeneous porous media," *J. Comput. Phys.*, vol. 477, Mar. 2023, Art. no. 111919.
[20] H. Ouyang, Z. Zhu, K. Chen, B. Tian, B. Huang, and J. Hao, "Reconstruction of hydrofoil cavitation flow based on the chain-style physics-informed neural network," *Eng. Appl. Artif. Intell.*, vol. 119, Mar. 2023, Art. no. 105724.
[21] M. Aliakbari, M. Mahmoudi, P. Vadasz, and A. Arzani, "Predicting high-fidelity multiphysics data from low-fidelity fluid flow and transport solvers using physics-informed neural networks," *Int. J. Heat Fluid Flow*, vol. 96, Aug. 2022, Art. no. 109002.

[22] A. Kumar, S. Ridha, M. Narahari, and S. U. Ilyas, "Physics-guided deep neural network to characterize non-Newtonian fluid flow for optimal use of energy resources," *Exp. Syst. Appl.*, vol. 183, Nov. 2021, Art. no. 115409.

[23] L. Li, Y. Li, Q. Du, T. Liu, and Y. Xie, "ReF-nets: Physics-informed neural network for Reynolds equation of gas bearing," *Comput. Methods Appl. Mech. Eng.*, vol. 391, Mar. 2022, Art. no. 114524.

[24] M. Raissi, P. Perdikaris, and G. E. Karniadakis, "Physics-informed neural networks: A deep learning framework for solving forward and inverse problems involving nonlinear partial differential equations," *J. Comput. Phys.*, vol. 378, pp. 686–707, Feb. 2019.

[25] M. Tancik, P. P. Srinivasan, B. Mildenhall, S. Fridovich-Keil, N. Raghavan, U. Singhal, R. Ramamoorthi, J. T. Barron, and R. Ng, "Fourier features let networks learn high frequency functions in low dimensional domains," in *Proc. Adv. Neural Inf. Process. Syst.*, 2020, pp. 7537–7547.

[26] D. Jiang, J. Sirignano, and S. N. Cohen, "Global convergence of deep Galerkin and PINNs methods for solving partial differential equations," 2023, *arXiv:2305.06000*.

[27] L. Lu, P. Jin, G. Pang, Z. Zhang, and G. E. Karniadakis, "Learning nonlinear operators via DeepONet based on the universal approximation theorem of operators," *Nature Mach. Intell.*, vol. 3, no. 3, pp. 218–229, Mar. 2021.

[28] S. Cuomo, V. S. Di Cola, F. Giampaolo, G. Rozza, M. Raissi, and F. Piccialli, "Scientific machine learning through physics–informed neural networks: Where we are and what's next," *J. Sci. Comput.*, vol. 92, no. 3, p. 88, Jul. 2022.

[29] A. Isaev, T. Dobroserdova, A. Danilov, and S. Simakov, "Physically informed deep learning technique for estimating blood flow parameters in four-vessel junction after the Fontan procedure," *Computation*, vol. 12, no. 3, p. 41, Feb. 2024.

[30] L. Fesser, L. D'Amico-Wong, and R. Qiu, "Understanding and mitigating extrapolation failures in physics-informed neural networks," 2023, *arXiv:2306.09478*.

[31] Y. Wang, Y. Yao, and Z. Gao, "An extrapolation-driven network architecture for physics-informed deep learning," 2024, *arXiv:2406.12460*.

[32] S. Cuomo, F. Giampaolo, S. Izzo, C. Nitsch, F. Piccialli, and C. Trombetti, "A physics-informed learning approach to Bernoulli-type free boundary problems," *Comput. Math. Appl.*, vol. 128, pp. 34–43, Dec. 2022.

[33] S. J. Raymond and D. B. Camarillo, "Applying physics-based loss functions to neural networks for improved generalizability in mechanics problems," 2021, *arXiv:2105.00075*.

[34] E. Kornaeva, A. Kornaev, and S. Egorov, "Application of artificial neural networks to solution of variational problems in hydrodynamics," *J. Phys., Conf.*, vol. 1553, no. 1, May 2020, Art. no. 012005.

[35] E. Kornaeva, A. Kornaev, A. Fetisov, I. Stebakov, and B. Ibragimov, "Physics-based loss and machine learning approach in application to non-Newtonian fluids flow modeling," in *Proc. IEEE Congr. Evol. Comput. (CEC)*, Jul. 2022, pp. 1–8.

[36] L. Milne-Thomson and N. Rott, "Theoretical hydrodynamics, fifth edition," *J. Appl. Mech.*, vol. 35, no. 4, p. 846, Dec. 1968.

[37] Y. Hori, *Hydrodynamic Lubrication*. Tokyo, Japan: Yokendo, 2006.

[38] S. V. Patankar, *Numerical Heat Transfer and Fluid Flow*, 1st ed., Boca Raton, FL, USA: CRC Press, Oct. 1980.

[39] N. E. Kochin, I. A. Kibel, and N. V. Roze, *Theoretical Hydromechanics*. New York, NY, USA: Interscience, 1964.

[40] A. Sequeira, *Hemorheology: Non-Newtonian Constitutive Models for Blood Flow Simulations*, vol. 2212. Berlin, Germany: Springer-Verlag, 2018, pp. 1–44.

[41] D. Rubin and E. Krempl, *Introduction To Continuum Mechanics*, 4th ed., Amsterdam, The Netherlands: Elsevier, 2010.

[42] G. A. Korn and T. M. Korn, *Mathematical Handbook for Scientists and Engineers: Definitions, Theorems, and Formulas for Reference and Review*. Little Falls, NJ, USA: Courier Corporation, 2000.

[43] L. Zheng and X. Zhang, "Exact analytical solutions for fractional viscoelastic fluids," in *Modeling and Analysis of Modern Fluid Problems*. Cambridge, MA, USA: Academic, Jan. 2017, pp. 279–359.

[44] G. Lu, X.-D. Wang, and Y.-Y. Duan, "A critical review of dynamic wetting by complex fluids: From Newtonian fluids to non-Newtonian fluids and nanofluids," *Adv. Colloid Interface Sci.*, vol. 236, pp. 43–62, Oct. 2016.

[45] I. Stebakov, A. Kornaev, E. Kornaeva, N. Litvinenko, Y. Kazakov, O. Ivanov, and B. Ibragimov, "Artificial neural networks as a natural tool in solution of variational problems in hydrodynamics [source code]," Tech. Rep., 2024. [Online]. Available: https://codeocean.com/capsule/7097126/tree/v1

[46] N. M. Wilson, A. K. Ortiz, and A. B. Johnson, "The vascular model repository: A public resource of medical imaging data and blood flow simulation results," *J. Med. Devices*, vol. 7, no. 4, Dec. 2013, Art. no. 040923.

[47] A. Updegrove, N. M. Wilson, J. Merkow, H. Lan, A. L. Marsden, and S. C. Shadden, "SimVascular: An open source pipeline for cardiovascular simulation," *Ann. Biomed. Eng.*, vol. 45, no. 3, pp. 525–541, Mar. 2017.

[48] F. Irgens, *Rheology and Non-Newtonian Fluids*. Berlin, Germany: Springer, Jul. 2013.

[49] M. Ashour, N. Valizadeh, and T. Rabczuk, "Phase-field Navier–Stokes model for vesicle doublets hydrodynamics in incompressible fluid flow," *Comput. Methods Appl. Mech. Eng.*, vol. 412, Jul. 2023, Art. no. 116063.

[50] O. Ronneberger, P. Fischer, and T. Brox, "U-Net: Convolutional networks for biomedical image segmentation," in *Proc. Int. Conf. Medical Image Comput. Comput.-Assist. Intervent.*, 2015, pp. 234–241.

[51] M. Buda, A. Saha, and M. A. Mazurowski, "Association of genomic subtypes of lower-grade gliomas with shape features automatically extracted by a deep learning algorithm," *Comput. Biol. Med.*, vol. 109, pp. 218–225, Jun. 2019.

[52] O. A. Catalano, A. H. Singh, R. N. Uppot, P. F. Hahn, C. R. Ferrone, and D. V. Sahani, "Vascular and biliary variants in the liver: Implications for liver surgery," *RadioGraphics*, vol. 28, no. 2, pp. 359–378, Mar. 2008.

[53] O. K. Baskurt, M. Boynard, G. C. Cokelet, P. Connes, B. M. Cooke, S. Forconi, F. Liao, M. R. Hardeman, F. Jung, H. J. Meiselman, G. Nash, N. Nemeth, B. Neu, B. Sandhagen, S. Shin, G. Thurston, and J. L. Wautier, "New guidelines for hemorheological laboratory techniques," *Clin. Hemorheol. Microcirculation*, vol. 42, no. 2, pp. 75–97, 2009.

[54] R. Revellin, F. Rousset, D. Baud, and J. Bonjour, "Extension of Murray's law using a non-Newtonian model of blood flow," *Theor. Biol. Med. Model.*, vol. 6, no. 1, pp. 1–9, Dec. 2009.

[55] M. M. Molla and M. C. Paul, "LES of non-Newtonian physiological blood flow in a model of arterial stenosis," *Med. Eng. Phys.*, vol. 34, no. 8, pp. 1079–1087, Oct. 2012.

[56] J. M. Jung, D. H. Lee, and Y. I. Cho, "Non-Newtonian standard viscosity fluids," *Int. Commun. Heat Mass Transf.*, vol. 49, pp. 1–4, Dec. 2013.

[57] P. K. Mandal, "An unsteady analysis of non-Newtonian blood flow through tapered arteries with a stenosis," *Int. J. Non-Linear Mech.*, vol. 40, no. 1, pp. 151–164, Jan. 2005.

[58] S. Wang, X. Yu, and P. Perdikaris, "When and why PINNs fail to train: A neural tangent kernel perspective," *J. Comput. Phys.*, vol. 449, Jan. 2020, Art. no. 110768.

[59] A. F. Psaros, K. Kawaguchi, and G. E. Karniadakis, "Meta-learning PINN loss functions," *J. Comput. Phys.*, vol. 458, Jun. 2022, Art. no. 111121.

[60] H. Son, S. W. Cho, and H. J. Hwang, "Enhanced physics-informed neural networks with augmented Lagrangian relaxation method (AL-PINNs)," *Neurocomputing*, vol. 548, Sep. 2023, Art. no. 126424.

IVAN STEBAKOV received the B.S. and M.S. degrees in mechatronics and robotics from Orel State University, Oryol, in 2018 and 2020, respectively.

Since 2020, he has been a Junior Researcher with the Scientific and Educational Center for Intelligent Technologies for Monitoring and Diagnostics of Power Generating Equipment, Orel State University. Since 2023, he has been a Researcher with the Laboratory of Artificial Intelligence in Medicine, Innopolis University. He is the author of 28 papers, including those in leading journals and conferences. His research interests include physics-informed machine learning, viscous fluid flows in complex channels, and intelligent diagnostics of rotor systems.

ALEXEI KORNAEV received the M.S. degree in mechanical engineering from the National University of Science and Technology "MISIS," Moscow, Russia, in 2003, the Ph.D. degree in engineering sciences (Eng.Sc.), in 2008, and the Dr.Habil. degree in Eng.Sc., in 2018.

From 2003 to 2013, he lectured with the National University of Science and Technology "MISIS," where he focused on the mechanics of continua and mathematical modeling. Since 2013, he has been a Senior Research Fellow and a Professor with Orel State University, leading projects in mathematical modeling and engineering. In 2020, he joined Innopolis University as a Research Fellow, specializing in AI applications in medicine and non-Newtonian fluid hydrodynamics. He is the author of more than 100 research papers, patents, and codes. His research interests include interpretable and trusted AI, physics-based machine learning, medical image and video processing, and non-Newtonian fluid dynamics.

ELENA KORNAEVA received the B.S. degree in applied mathematics from the National University of Science and Technology "MISIS," Stary Oskol, Russia, in 2008, and the Ph.D. degree in mathematical modeling, numerical methods, and software engineering from Yelets State University, Yelets, Russia, in 2011.

From 2008 to 2013, she was a Lecturer and then a Senior Lecturer with the National University of Science and Technology "MISIS." Since 2013, she has been an Associate Professor with the Department of Information Systems and Digital Technologies, Orel State University. Her research interests include mathematical modeling of hydrodynamic processes, machine learning, and deep learning.

NIKITA LITVINENKO received the B.S. degree in computer science from Far East Federal University, in 2012, and the M.S. degree in applied mathematics from Tomsk State University, in 2022. He is currently pursuing the Ph.D. degree with Innopolis University. He is working on his Ph.D. thesis, which focuses on the application of cross-modal deep learning models for software bug detection and correction.

From 2022 to 2024, he was a Research Assistant with Innopolis University. His research interests include AI and machine learning applications in natural language processing and software engineering.

Mr. Litvinenko joined a team that was awarded the MTS AI Grant to enhance the performance of large language models, in 2024.

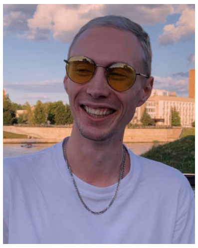

YURI KAZAKOV received the B.S. and M.S. degrees in mechatronics from Orel State University, Oryol, Russia, in 2021 and 2023, respectively.

Since 2019, he has been a Research Fellow with Orel State University, specializing in fluid dynamics, AI, and machine learning applications in engineering. He has contributed to the study of fluid film bearings using artificial intelligence. His work encompasses the use of AI for detecting bearing faults, controlling mechanical systems, and generating artificial data. He has published more than 60 research works, including papers in top-tier journals and conferences. His research interests include non-Newtonian fluid hydrodynamics and intelligent control systems for rotating machines. He also takes an active part in scientific projects and conducts scientific research.

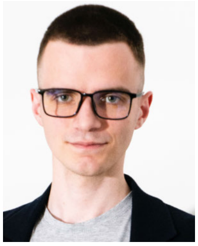

OLEG IVANOV received the B.S. degree in automotive engineering from Orel State University, Oryol, Russia, in 2023. He is currently pursuing the M.S. degree in data science with ITMO University, Saint Petersburg, Russia.

Since 2024, he has been with the Research Center for Artificial Intelligence, Innopolis University, Innopolis, Russia, where he engages in research and development projects. As a Student, he has been involved in several research activities focusing on deep learning, natural language processing, and computer vision. His work includes contributions to publications in journals and conference proceedings, reflecting his growing expertise in these areas.

BULAT IBRAGIMOV received the B.S. and M.S. degrees in computer science from Kazan Federal University, Republic of Tatarstan, in 2010, and the Ph.D. degree from the University of Ljubljana, in 2014.

From 2016 to 2018, he was a Postdoctoral Fellow with the Department of Radiation Oncology, Stanford University. From 2018 to 2019, he was a Senior Research Scientist with Auris Health (Johnson and Johnson). Currently, he is an Associate Professor with the Department of Computer Science, University of Copenhagen, Denmark. His research interests include machine learning in medicine, computer-aided diagnosis, medical image analysis, and human–AI interaction.

Dr. Ibragimov received various awards, including the Novo Nordisk Award for Young Data Science Investigator.